Mon. Not. R. Astron. Soc. **280**, 863–867 (1996)

# Ultra-high-resolution measurements of the intrinsic line profiles of interstellar $C_2$ towards $\zeta$ Ophiuchi and HD 169454

I. A. Crawford and M. J. Barlow

*Department of Physics and Astronomy, University College London, Gower Street, London WC1E 6BT*



Accepted 1995 December 21. Received 1995 December 13; in original form 1995 October 18

## ABSTRACT

We have used the Ultra-High-Resolution Facility at the Anglo-Australian Telescope (AAT), operating at a resolution of 0.35 km $s^{-1}$ (FWHM), to measure the intrinsic profiles of the Q(2) and Q(4) lines of the (2–0) Phillips band of interstellar $C_2$ towards $\zeta$ Oph and HD 169454. The $C_2$ lines were found to be very narrow, with intrinsic velocity dispersions ($b$-values) in the range 0.25–0.71 km $s^{-1}$. In the case of $\zeta$ Oph, two velocity components (separation $1.10 \pm 0.17$ km $s^{-1}$) have been resolved, and found to have rather different linewidths and rotational excitation temperatures. In the case of HD 169454, the data are consistent with a single velocity component, but the well-defined $b$-value ($0.59 \pm 0.04$ km $s^{-1}$) and low kinetic temperature would then imply supersonic turbulent velocities. One way to avoid this conclusion is to postulate the existence of unresolved velocity structure (or a velocity gradient) within the cloud.

**Key words:** line: profiles – stars: individual: $\zeta$ Oph – stars: individual: HD 169454 – ISM: molecules.

## 1 INTRODUCTION

The Ultra-High-Resolution Facility (UHRF) at the Anglo-Australian Telescope (AAT) has now fulfilled its potential to make advances in our understanding of the interstellar medium through its ability to resolve the intrinsic profiles of interstellar absorption lines (e.g. Crawford et al. 1994; Barlow et al. 1995; Crawford 1995; Sarre et al. 1995). Here, we report the use of this instrument, which has been described in detail by Diego et al. (1995), to make the first ever measurements of the intrinsic line profiles of interstellar $C_2$ molecules. The main aim was to quantify the extent to which diffuse molecular clouds are turbulent in the regions where $C_2$ occurs.

The velocity dispersion, $b$, of an interstellar line is related to the kinetic temperature, $T_k$, and the rms turbulent velocity, $v_t$, by the expression

$$b = \left(\frac{2kT_k}{m} + 2v_t^2\right)^{1/2}, \qquad (1)$$

where $k$ is Boltzmann's constant, and $m$ is the mass of the atom or molecule observed. As the kinetic temperature, $T_k$, can in principle be determined from the rotational excitation of the $C_2$ molecule (van Dishoeck & Black 1982), equation (1) can be used to determine $v_t$ directly, provided that $b$ is accurately measured by means of high-resolution spectroscopy.

## 2 OBSERVATIONS

Observations of the Q(2) and Q(4) lines of the (2–0) Phillips band of $C_2$, which occurs near 8760 Å, were obtained with the UHRF in 1995 July. A summary of the observations is given in Table 1. The detector was the AAO Tektronix CCD (1024 × 1024 24-μm pixels), and the spectrograph was operated with a confocal image slicer (Diego 1993). The CCD output was binned by a factor of 8 perpendicular to the dispersion direction in order to reduce the readout noise associated with extracting the broad spectrum produced by the slicer. The resolution, measured from the observed width of a stabilized He–Ne laser line, was $0.35 \pm 0.01$ km $s^{-1}$ (FWHM), corresponding to a resolving power of $R = 860000$. Other aspects of the instrument and observing procedures have been described in detail by Barlow et al. (1995) and Diego et al. (1995).

The CCD images were divided by a flat-field, and the spectra were extracted using the FIGARO data reduction package (Shortridge 1988) at the UCL Starlink node. Scattered light was measured from the interorder region and subtracted. Wavelength calibration was performed using a Th–Ar lamp. Once wavelength-calibrated, the spectra were converted to the heliocentric velocity frame [adopting rest wavelengths of 8761.194 and 8763.751 Å for the Q(2) and Q(4) lines, respectively, as tabulated by van Dishoeck &de Zeeuw 1984].

Multiple exposures (Table 1) were co-added, and the resulting spectra were normalized by division of low-order polynomial fits to the continua on either side of the absorption lines. The normalized spectra are shown in Fig. 1.

## 3 DISCUSSION

The primary aim of the present work was to determine the intrinsic linewidths of the interstellar $C_2$ lines, and to this end least-squares Gaussian fits were performed on the observed profiles using the DIPSO spectral reduction package (Howarth, Murray & Mills 1993). The fits are shown superimposed on the data in Fig. 1, and the resulting line profile parameters are given in Table 2. Table 2 also gives the column densities of the $J=2$ and $J=4$ rotational levels, derived from the measured equivalent widths and the band oscillator strength ($f_{20}=1.0\times10^{-3}$) recommended by van Dishoeck & Black (1989); adoption of the somewhat larger oscillator strength ($1.36\pm0.15\times10^{-3}$) obtained recently by Erman & Iwamae (1995) would cause these column densities to be reduced by 36 per cent.

In reality, both the Q(2) and Q(4) lines must have the same velocity dispersion, so the weighted mean $b$-values have been calculated for each velocity component, and these values are listed in Table 3. Also given in Table 3 are the rigorous upper limits to the kinetic temperatures for each component (i.e., the values deduced from the line profiles on the assumption that there is no line-of-sight turbulence), and the rotational excitation temperatures based on the populations of the $J=2$ and $J=4$ levels.

As discussed in detail by van Dishoeck & Black (1982), the ground-state rotational levels of $C_2$ are populated by a combination of collisional and radiative processes. This means that the populations cannot, in general, be described by a single excitation temperature, and although the rotational temperatures deduced from the lower-lying levels more closely approximate the kinetic temperature than those from higher levels, these still overestimate the true kinetic temperature of the gas.

Owing to bad weather at the telescope, only the Q(2) and Q(4) lines towards ζ Oph and HD 169454 were observed here, so a full rotational excitation analysis based on the

**Table1.** List of observations made of interstellar $C_2$ lines towards ζ Oph and HD 169454. Many of the observations were through cloud, so these exposure times and count levels do not give a true indication of the instrumental efficiency.

| Star | $V$ | $I$ | $E(B-V)$ | Line | Exposures ($n\times$ secs) | Counts ($e^-$) |
|---|---|---|---|---|---|---|
| ζ Oph | 2.6 | 2.5 | 0.33 | Q(2) | 6 × 1200 | $4.2\times10^4$ |
| | | | | Q(4) | 4 × 1200 | $2.4\times10^4$ |
| 169454 | 6.6 | 4.8 | 1.14 | Q(4) | 3 × 1200 | $2.0\times10^3$ |
| | | | | Q(2) | 3 × 1200 | $2.0\times10^3$ |

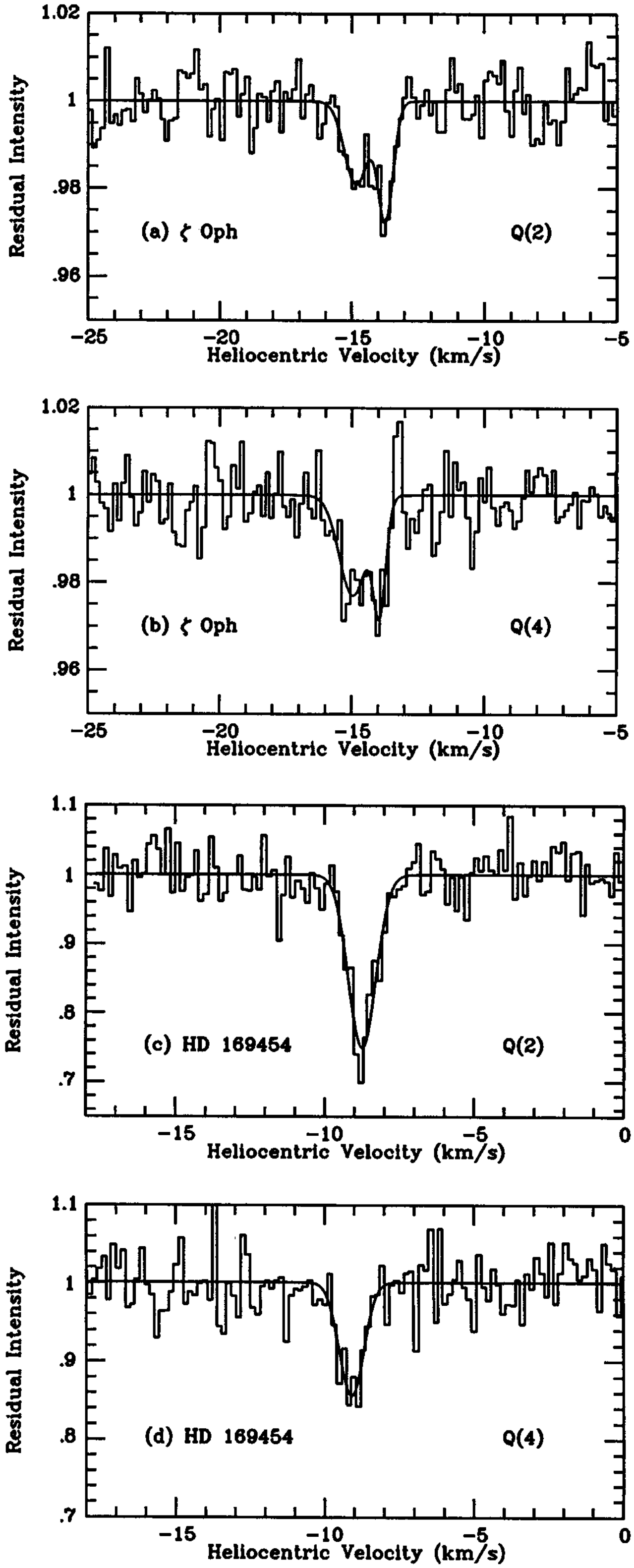


**Figure 1.** The interstellar $C_2$ lines observed towards ζ Oph and HD 169454. The observed data are plotted as histograms. The smooth curves are least-squares Gaussian fits with the velocity dispersions given in Table 2.

**Table 2.** Line profile parameters determined for the Q(2) and Q(4) lines towards ζ Oph and HD 169454. $(\Delta v)_{obs}$ is the observed FWHM (determined by least-squares Gaussian fitting; $1\sigma$ errors), and $b$ is the corresponding intrinsic line velocity dispersion (i.e., after deconvolving the instrumental resolution); $w_\lambda$ is the measured equivalent width ($2\sigma$ errors), and $N$ is the column density, deduced from the equivalent widths.

| Star | Line | $v_{helio}$ (km s$^{-1}$) | $(\Delta v)_{obs}$ (km s$^{-1}$) | $b$ (km s$^{-1}$) | $w_\lambda$ (here) (mÅ) | $w_\lambda$ (other) (Ref) (mÅ) | $N$ (cm$^{-2}$) |
|---|---|---|---|---|---|---|---|
| ζ Oph | Q(2) | $-14.83 \pm 0.15$ | $1.05 \pm 0.37$ | $0.59 \pm 0.22$ | $0.55 \pm 0.15$ | }$1.2 \pm 0.3$ (1); $1.1 \pm 0.1$ (2) | $(1.62 \pm 0.44) \times 10^{12}$ |
| | | $-13.73 \pm 0.08$ | $0.68 \pm 0.18$ | $0.35 \pm 0.11$ | $0.61 \pm 0.14$ | | $(1.79 \pm 0.41) \times 10^{12}$ |
| | Q(4) | $-14.95 \pm 0.13$ | $1.24 \pm 0.28$ | $0.71 \pm 0.17$ | $0.84 \pm 0.19$ | }$1.5 \pm 0.3$ (1); $1.7 \pm 0.2$ (2) | $(2.47 \pm 0.56) \times 10^{12}$ |
| | | $-13.95 \pm 0.07$ | $0.55 \pm 0.12$ | $0.25 \pm 0.07$ | $0.48 \pm 0.17$ | | $(1.41 \pm 0.50) \times 10^{12}$ |
| 169454 | Q(2) | $-8.73 \pm 0.04$ | $1.08 \pm 0.09$ | $0.61 \pm 0.05$ | $8.14 \pm 1.18$ | $8.0 \pm 1.2$ (3); $6.6 \pm 0.8$ (4) | $(2.39 \pm 0.35) \times 10^{13}$ |
| | Q(4) | $-9.10 \pm 0.06$* | $0.96 \pm 0.15$ | $0.54 \pm 0.09$ | $3.98 \pm 1.03$ | $5.0 \pm 0.8$ (3); $5.9 \pm 0.7$ (4) | $(1.17 \pm 0.30) \times 10^{13}$ |

*Velocity uncertain due to the detection of only one comparison line in the Th–Ar comparison lamp spectrum. References. (1) Hobbs & Campbell (1982); (2) Danks & Lambert (1983); (3) Gredel & Münch (1986); (4) van Dishoeck & Black (1989).

**Table 3.** The weighted mean velocity dispersions ($\bar{b}$) of each identified velocity component, together with the corresponding upper limit to the kinetic temperature, $T_k^{ul}$, based on the assumption that turbulence does not contribute to the observed line widths. $T_{42}$ is the rotational excitation temperature based on the relative populations of the $J=2$ and 4 rotational levels, $T_k$ (vDB) is the kinetic temperature deduced by van Dishoeck & Black (1986, 1989), $C_s$ is the sound speed at the adopted kinetic temperatures, and $v_t$ is the rms turbulent velocity along the line of sight, obtained from the observed linewidths, assuming the kinetic temperatures found by van Dishoeck & Black.

| Star | $v_{helio}$ (km s$^{-1}$) | $\bar{b}$ (km s$^{-1}$) | $T_k^{ul}$ (K) | $T_{42}$ (K) | $T_k$ (vDB) (K) | $C_s$ (km s$^{-1}$) | $v_t$ (km s$^{-1}$) |
|---|---|---|---|---|---|---|---|
| ζ Oph | $-14.8$ | $0.67 \pm 0.14$ | $650 \pm 270$ | $220^{+\infty}_{-160}$ | $30 \pm 10$ | $0.33^{+0.05}_{-0.06}$ | $0.46 \pm 0.10$ |
| | $-13.7$ | $0.28 \pm 0.06$ | $110 \pm 50$ | $44^{+34}_{-18}$ | $30 \pm 10$ | $0.33^{+0.05}_{-0.06}$ | $0.17 \pm 0.05$ |
| 169454 | $-8.7$ | $0.59 \pm 0.04$ | $510 \pm 70$ | $28^{+7}_{-6}$ | $15^{+10}_{-5}$ | $0.23^{+0.07}_{-0.04}$ | $0.41 \pm 0.03$ |

UHRF data has not been possible. However, such an analysis has been performed for these two stars, albeit on the basis of lower resolution data, by van Dishoeck & Black (1986, 1989), and the kinetic temperatures deduced by them are reproduced in Table 3. Recently, on the basis of *Hubble Space Telescope* (*HST*) observations of the Mulliken (0–0) band of $C_2$ at 2313 Å, Lambert, Sheffer & Federman (1995) have obtained a temperature for the ζ Oph cloud ($20 < T_k < 45$ K) which is essentially identical to the value ($30 \pm 10$ K) found by van Dishoeck & Black (1986). It will be seen from Table 3 that, as expected, the excitation temperatures deduced from the $J=2$ and $J=4$ levels are somewhat higher than these kinetic temperatures. Of course, van Dishoeck & Black (1986, 1989) and Lambert et al. (1995) did not resolve the two velocity components towards ζ Oph, which might in principle have different kinetic temperatures (see below).

By combining the kinetic temperatures found by van Dishoeck & Black with the intrinsic linewidths measured with the UHRF, it is possible to make a fairly accurate determination of the turbulent velocity in the region of each cloud containing the $C_2$ molecules. The last column in Table 3 lists the turbulent velocities derived using equation (1) for each velocity component. For comparison, Table 3 also gives the speed of sound at the adopted kinetic temperatures, derived under the assumption of a molecular hydrogen gas (assumed to contain 10 per cent helium by number relative to hydrogen nuclei).

We now turn to a more detailed discussion of each of the two sightlines.

### 3.1 ζ Oph

The present observations have clearly resolved the two velocity components detected previously in CH and CN (Lambert, Sheffer & Crane 1990; Crawford et al. 1994), and the velocity separation of these components ($1.10 \pm 0.17$ km s$^{-1}$; Table 2) is identical to that ($1.13 \pm 0.10$ km s$^{-1}$) found for the other molecules. This is the first time that this velocity structure has been resolved in $C_2$, but we note that the sun of the equivalent widths of the two components agree very well with the values obtained at lower resolution by other authors (Table 2).

The data presented here suggest that the physical conditions in these two clouds may be somewhat different. The most important evidence for this is the higher excitation temperature of the $-14.8$ km s$^{-1}$ component (Table 3). As noted above, we expect the excitation temperature derived from the low-lying rotational levels to be of the same order as, but somewhat higher than, the actual kinetic temperature in the gas. This condition is fulfilled for the $-13.7$ km s$^{-1}$ component if we adopt the kinetic temperature of $30 \pm 10$ K deduced by van Dishoeck & Black (1986). However, even allowing for the large errors, we see that the excitation temperature of the $-14.8$ km s$^{-1}$ component appears to be significantly higher, which almost certainly indicates a higher kinetic temperature. In addition, the fact that the $-14.8$ km s$^{-1}$ component is significantly broader than the $-13.7$ km s$^{-1}$ component supports the suggestion of a higher kinetic temperature: the width of the $-14.8$ km s$^{-1}$ component implies marginally supersonic turbulence at a temperature of 30 K (Table 3), but a higher temperature would imply a lower, and perhaps more physically realistic, turbulent velocity. It is true that the larger $b$-value of this component might be due to still unresolved velocity structure (as we discuss below in the context of the relatively broad component towards HD 169454), but this would not account for its apparently higher excitation temperature.

Given that $\zeta$ Oph is a standard sightline for testing physical and chemical models if interstellar clouds, and that previous analyses have been based on the assumption of a single molecular cloud, it is clearly important to determine the extent to which the physical conditions in these two velocity components are different. This will necessitate the observation of lines from many more rotational levels, so that a full excitation analysis can be performed for each component, and we hope to obtain such observations in the near future.

### 3.2 HD 169454

For the line of sight towards HD 169454 only one $C_2$ velocity component is present, and the various line profile and physical parameters are therefore well defined (Tables 2 and 3). Van Dishoeck & Black (1989) deduced a very low kinetic temperature ($15^{+10}_{-5}$ K) on the basis of a full rotational analysis, and we see that this is fully consistent with (i.e., is of the same order as, but slightly lower than) the excitation temperature derived from the $J=2$ and 4 rotational levels.

One consequence of this low kinetic temperature is an apparently supersonic turbulent velocity. Whereas in the case of the $-14.8$ km s$^{-1}$ component towards $\zeta$ Oph the turbulent velocity is only marginally supersonic, and there are indications (discussed above) that a higher kinetic temperature would make the observed linewidth consistent with subsonic turbulence, no such explanation is possible for the cloud towards HD 169454. The well-defined temperature and velocity dispersion (Table 3) ensure that $v_t$, as defined by equation (1), is significantly greater than the local sound speed. Thus, either the turbulence is genuinely supersonic, which would almost certainly imply an active energy source within the cloud, or the assumptions underlying equation (1) are incorrect. The weakest of these assumptions is that the bulk motions in the line of sight have a Gaussian distribution of velocities (with standard deviation, $v_t$), and that no unresolved velocity structure, or velocity gradient, is present.

**Table 4.** Line profile parameters for a two-component fit to the $C_2$ Q(2) line towards HD 169454 (see text for discussion).

| $v_{helio}$ (km s$^{-1}$) | $b$ (km s$^{-1}$) | $\log N$ (cm$^{-2}$) |
|---|---|---|
| $-8.9 \pm 0.1$ | $0.30^{+0.10}_{-0.05}$ | $13.30^{+0.10}_{-0.05}$ |
| $-8.2 \pm 0.1$ | $0.30^{+0.10}_{-0.10}$ | $12.90^{+0.10}_{-0.30}$ |

The cloud towards HD 169454 has been mapped in CO emission by Jannuzi et al. (1988), and is found to have a diameter of 20 arcmin (corresponding to 0.7 pc at an estimated distance of 125 pc[1]). The maps reveal the presence of three relatively dense clumps, approximately 0.15 pc across, connected by lower intensity emission. The line of sight to the star passes approximately 5.7 arcmin (0.21 pc) south–south-west of the centre of one of these clumps (Clump B in fig. 1 of Jannuzi et al.).

Given this complicated internal structure, and the fact that Jannuzi et al. found radial velocity differences of 0.5 to 1 km s$^{-1}$ between clumps, we might expect additional unresolved velocity structure to be present through the cloud. Indeed, Jannuzi et al. noted that asymmetries in their $^{13}$CO line profiles 'provide weak evidence of multiple velocity components along the line of sight', and close inspection of the Q(2) line (Fig. 1c) does reveal an asymmetry (in the form of a slightly shallower red wing) similar to that found in the radio data (cf. fig. 6a of Jannuzi et al. 1988).

In order to determine whether velocity substructure might account for the observations without the need to invoke supersonic turbulence, two-component theoretical line profiles were calculated using the interstellar routines in the DIPSO program (Howarth et al. 1993) and compared with the observed line profiles. The results of a two-component fit are given in Table 4, and the best-fitting profile is shown superimposed on the observations in Fig. 2.

Table 4 shows that the Q(2) line towards HD 169454 can be well fitted by two velocity components separated by 0.7 km s$^{-1}$. Each component would then have a $b$-value of only 0.3 km s$^{-1}$, and a subsonic turbulent velocity of 0.2 km s$^{-1}$. While higher signal-to-noise observations will be needed to prove unequivocally that such velocity structure is present, this analysis indicates this to be a plausible alternative to supersonic turbulence.

Another possibility would be the existence of a smooth velocity gradient within the cloud. Recently, Linsky et al. (1995) have used *HST* observations of interstellar H I and D I towards Capella and Procyon to derive the kinetic tem-

[1]Jannuzi et al. consider two possibilities for the distance: 125 and 750 pc. We adopt the former value because, for the reasons set out in section 4.1 of Crawford (1992), we consider it most likely that this cloud is associated with the local ridge of molecular clouds mapped by Dame et al. (1987; their fig. 7), rather than lying significantly in the background.

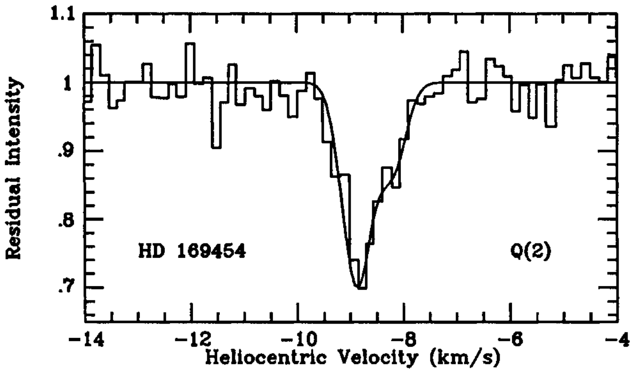


**Figure 2.** A two-component fit to the Q(2) line towards HD 169454 with the line profile parameters given in Table 4.

peratures and (subsonic) turbulent velocity dispersions for the warm neutral gas towards these stars. They raised the question of whether the derived 'turbulent' motions might be due to smooth velocity gradients within the gas rather than to random turbulence. Similarly, the necessity for supersonic turbulent motions in the sightline towards HD 169454 could be avoided by postulating the existence such a velocity gradient. This would give rise to an asymmetric, but smooth, absorption profile. Sufficiently high signal-to-noise UHRF observations should be capable of distinguishing such a profile from one broadened by random turbulence, or from one due to two discrete absorbing components.

## 4 CONCLUSIONS

We have resolved the intrinsic profiles of the $C_2$ Q(2) and Q(4) lines towards ζ Oph and HD 169454. In all cases the $C_2$ lines were found to be very narrow, with intrinsic velocity dispersions (*b*-values) in the range 0.25–0.71 km $s^{-1}$ (Table 2).

In the case of ζ Oph, both velocity components (separation $1.10 \pm 0.17$ km $s^{-1}$) have been resolved, and found to have rather different linewidths and rotational excitation temperatures (Table 3). While the $-13.8$ km $s^{-1}$ component has a linewidth and excitation temperature consistent with a kinetic temperature of 30 K (van Dishoeck & Black 1986), and clearly subsonic turbulence, the $-14.8$ km $s^{-1}$ component is almost certainly hotter and (depending on what the temperature actually turns out to be) probably more turbulent. It is important to obtain observations of lines from significantly more rotational levels, so that a full excitation analysis can be performed for each velocity component.

In the case of HD 169454, the present data are consistent with a single velocity component, but in this case the well-defined *b*-value and temperature (Table 3) would imply supersonic turbulent velocities. One way to avoid this conclusion is to postulate the existence of unresolved velocity structure (or a velocity gradient) within the cloud, and we show (Figure 2 and Table 4) that two subcomponents (with *b*-values of 0.3 km $s^{-1}$ and separated by 0.7 km $s^{-1}$) are capable of explaining the observed Q(2) line profile without the need to introduce supersonic velocities. There is some evidence, in the form of asymmetric $^{13}CO$ line profiles, for such substructure in the molecular cloud towards this star (Jannuzi et al. 1988), but higher signal-to-noise observations will be required to confirm it in the $C_2$ lines.

## ACKNOWLEDGEMENTS

We thank Sean Ryan at the AAO for his help in locating the echelle orders containing the $C_2$ lines, and PATT for the award of telescope time. IAC is grateful to PPARC for the award of a Post-Doctoral Research Fellowship.

## REFERENCES

Barlow M. J., Crawford I. A., Diego F., Dryburgh M., Fish A. C., Howarth I. D., Spyromilio J., Walker D. D., 1995, MNRAS, 272, 333
Crawford I. A., 1992, MNRAS, 254, 264
Crawford I. A., 1995, MNRAS, 277, 458
Crawford I. A., Barlow M. J., Diego F., Spyromilio J., 1994, MNRAS, 266, 903
Dame T. M. et al., 1987, ApJ, 322, 706
Danks A. C., Lambert D. L., 1983, A&A, 124, 188
Diego F., 1993, Applied Optics, 32, 6284
Diego F. et al., 1995, MNRAS, 272, 323
Erman P., Iwamae A., 1995, ApJ, 450, L31
Gredel R., Münch G., 1986, A&A, 154, 336
Hobbs L. M., Campbell B., 1982, ApJ, 254, 108
Howarth I. D., Murray J., Mills D., 1993, Starlink User Note No. 50, Rutherford Appleton Laboratory
Jannuzi B. T., Black J. H., Lada C. J., van Dishoeck E. F., 1988, ApJ, 332, 995
Lambert D. L., Sheffer Y., Crane P., 1990, ApJ, 359, L19
Lambert D. L., Sheffer Y., Federman S. R., 1995, ApJ, 438, 740
Linsky J. L., Diplas A., Wood B E., Brown A., Ayres T. R., Savage B. D., 1995, ApJ, 451, 335
Sarre P. J., Miles J. R., Kerr T. H., Hibbins R. E., Fossey S. J., Somerville W. B., 1995, MNRAS, 277, L41
Shortridge K., 1988, Starlink Users Note No. 86, Rutherford Appleton Laboratory
van Dishoeck E. F., Black J. H., 1982, ApJ, 258, 533
van Dishoeck E. F., Black J. H., 1986, ApJ, 307, 332
van Dishoeck E. F., Black J. H., 1989, ApJ, 340, 273
van Dishoeck E. F., de Zeeuw T., 1984, MNRAS, 206, 383